



## Chemical Modification and Characterization of Chitosan for Pharmaceutical Applications

Mohammed A. Almualla<sup>1\*</sup>, Mazin N. Mousa<sup>1</sup>, Mohammed Sattar<sup>2</sup>,



<sup>1</sup> Department of Pharmaceutical Chemistry, College of Pharmacy, Basra University, Basra, Iraq.

<sup>2</sup> Department of Pharmaceutics, College of Pharmacy, Basra University, Basra, Iraq.

### Abstract

Nine crosslinked chitosan derivatives (CLCS) were prepared using three different types of crosslinkers: glutaraldehyde, glyoxal and terephthaldehyde. The prepared CLCS were used to control the acyclovir (ACV) release in order to improve its oral bioavailability. The CLCS were prepared by Schiff based reaction and characterized by means of infrared spectroscopy (FTIR), x-ray diffraction measurements, thermogravimetric inspection, differential scanning calorimetry, and scanning electron microscopy (SEM). Establishment of an imine (C=N) bond was evidenced in FTIR. Compared to raw chitosan, the crosslinked chitosan derivatives showed more amorphous structure and exhibited more water holding capacity that increased with raising the crosslinking percent. In SEM, the CLCS demonstrated areas with rough surfaces and grooves that did not present in the smooth chitosan surface. The difference in swelling degree with varying crosslinker amount was also examined. The crosslinked chitosan displayed less swelling, and the degree of swelling decreased with increasing the density of crosslinking agent. The CLCS investigated in controlling the release of acyclovir by being incorporated with ACV in granules formulations. *In vitro* drug release results exhibited sustained release of ACV affected by the type and percent of crosslinker.

**Keywords:** Chitosan, crosslinked chitosan, Schiff base, glyoxal, glutaraldehyde, terephthaldehyde, sustained release.

### 1. Introduction

Polymeric materials, extending from natural to synthetic, had gained great attention in recent years at various everyday life applications. However, natural renewable polymers are preferred over their synthetic rivals as serve a variety of benefits especially regarding their sustainability, environmental friendliness, and ease of processing. Among diverse renewable biopolymers, chitosan (CS) is regarded as one of the greatest commercially prominent biocompatible macromolecules from biomedical or environmental considerations [1].

Chitosan is a semi-synthetic aminopolysaccharide originally derived from the natural biopolymer chitin by deacetylation. After cellulose, Chitin is the most abundant renewable polysaccharide within the marine environment and one among the most abundant polymer in the world [2]. The discovery of chitin and

chitosan emerged with the work of Henry Braconnot at 1811 [3], Odier in 1823 [4], and Rouget in 1859 was the first who discover the chitosan entity [5].

Distinguished features afford chitosan massive recognition in compare to synthetic polymers at applied research and practical applications [6]. Chitosan has exceptional macromolecular construction. Moreover, chitosan is well known as a biocompatible, nontoxic, bioactive, and biodegradable biopolymer [7, 8].

However, chitosan has some drawbacks especially those regarded to the pH-dependent solubility and degradation in acidic solutions. These problems limit CS applications as a drug delivery matrix [9]. Various physical and chemical approaches have been developed to modify CS physicochemical features and widen its applications [10]. Three types of reactive functional groups are present in CS macromolecule which are the hydroxyl (primary and secondary) sets at C-3 and C-6 positions, and the amino group

\*Corresponding author e-mail: [dr.mohammad\\_adil@yahoo.com](mailto:dr.mohammad_adil@yahoo.com); (Mohammed A. Almualla).

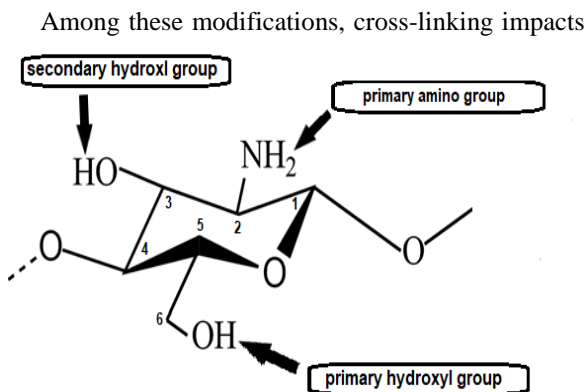
Receive Date: 06 February 2021, Revise Date: 07 March 2021, Accept Date: 21 March 2021

DOI: 10.21608/EJCHEM.2021.61809.3331

©2021 National Information and Documentation Center (NIDOC)

(primary) at C-2 position [11] as exhibited in Figure 1. These groups give chitosan the opportunity for assorted chemical modifications.

Fig. 1. Functional groups of chitosan



valuable properties for instance chemical stability, inherent mechanical strength, swelling capability, solubility, and drug release modifying aspects of chitosan. Cross-linked chitosan derivatives (CLCS) show pH-adaptive swelling tendency with hindered solubility adding on their own porous structure, the loaded drug can be released from CLCS by swelling of the chitosan matrix on the gastric acidic pH and drug diffusion through the pores in a sustained release manner. These unique features can be invested in innovative drug delivery formulations [12]. Dialdehydes are among crosslinkers employed to ameliorate chitosan features [13]. Compared to other crosslinkers, the use of dialdehydes as bifunctional crosslinkers creates a three-dimensional macromolecular network and turns chitosan structures more stable and resistant to acidic media by securing the chitosan amino groups with preserving the chitosan primary structure.

Acyclovir (9-[(2-hydroxyethoxy) methyl]-9H-guanine), is the prototype antiviral drug utilized to treat different types of herpes simplex viral infections. Inadequate oral absorption and short biological half-life of acyclovir (2 to 3 hours) asked for frequent dosing. There are many approaches to improve the oral bioavailability and sustain the release of acyclovir [14, 15].

This work aims to prepare crosslinked chitosan using three types of dialdehydes (glutaraldehyde, glyoxal, and terephthaldehyde) based on the Schiff base reaction. Additionally, the aim of the work is extended to investigate the release behavior of ACV from the prepared CLCS.

## 2. Experimental

### 2.1 Materials

Chitosan (CS), Glutaraldehyde (GU), and Glyoxal (GX) were purchased from Sigma-Aldrich/Germany. Terephthaldehyde (TP) was supplied from Merck KGaA, Darmstadt, Germany. Acyclovir (ACV) was provided from Zhejiang medicines and health products import and export Co. LTD., China. Glacial acetic acid was obtained from HiMedia Laboratories Pvt. Ltd., Mumbai, India. Hydrochloric acid (HCl) was got from ROMIL Ltd, The Source Convent Drive, Water beach, Cambridge. Sodium Carbonate ( $\text{Na}_2\text{CO}_3$ ) was purchased from Thomas Baker (Chemicals) Pvt. Ltd., Mumbai, India.

### 2.2 Procedures

#### 2.2.1 Preparation of cross-linked chitosan (CLCS)

Crosslinked chitosan derivatives were prepared by adding the crosslinker to chitosan. Chitosan (CS) was dispersed in a sufficient quantity of glacial acetic acid (AC) with stirring for 12 hours (hr) to ensure uniform suspension. Three types of crosslinkers were utilized in this study to react with chitosan individually: glyoxal, glutaraldehyde, and terephthaldehyde with three different percentages of crosslinking (12 %, 6%, and 3%) for each crosslinker were done to assess the crosslinking ratio effect on the chitosan properties. Accordingly, nine products of CLCS were prepared.

Glyoxal (GX) was dispersed in 40% weight (wt) in water solution from which diluted glyoxal solution 2% was prepared using glacial AC for easily handling. Volume of 0.87 milliliters (ml) from 2% GX solution was employed to crosslink 1 g of chitosan to 12%-degree, 0.435 ml for 6% crosslinking, and 0.217 ml for 3% crosslinking. Glutaraldehyde (GU) 2.5% solution was prepared from the available 25 % product. For 3%, 6%, and 12% crosslinking of chitosan with glutaraldehyde, volumes of 0.3 ml, 0.6 ml, and 1.2 ml from 2.5 % glutaraldehyde solution for each 1 g of chitosan were added to CS suspension. Terephthaldehyde (TP) was present in solid form. A solution of 2% terephthaldehyde was prepared by dissolving 0.4 g of TP in 20 ml of glacial AC. For 12 %, 6 %, and 3% cross-linking, 2 ml, 1 ml, and 0.5 ml from the solution were taken respectively to crosslink 1 g of chitosan. The calculated volumes of the crosslinkers solutions were added gradually to chitosan suspension drop by drop with continuous stirring using a magnetic stirrer for 6 hours. Refluxed at 60°C until cross-linked chitosan gel was formed which precipitated out from the suspension. The

suspension was then filtered to get the gel using wetted filter paper. After filtration, drops of 5% Sodium carbonate ( $\text{Na}_2\text{CO}_3$ ) were added on the remnant in the filter paper to remove acetic acid (neutralization) until the end of effervescence which indicates the reaction between glacial acetic acid and carbonate with the release of carbon dioxide ( $\text{CO}_2$ ). The products were washed thoroughly with distilled water (D.W.) several times to remove salts and any unreacted particles then left to dry at room temperature for 24 hours, then at 50 °C in the oven for 30 minutes to ensure complete drying. Grinding to get uniform powder was done and saved in closed containers.

### 2.2.2 Identification of Acyclovir (ACV)

#### -Determination of melting point

To determine purity, the melting point of acyclovir was defined using the capillary tube method. The vessel (closed from one end) was loaded to 2-3 mm with the drug powder, tapped, and placed within the melting point apparatus. The sample was observed within the apparatus and the temperature at which the drug powder turned into liquid was recorded as the melting point [16].

#### -Estimation of a calibration curve

For the estimation of acyclovir concentration using UV spectrophotometry, a calibration curve of acyclovir in 0.1N HCl was provoked. Standard solution of drug 150  $\mu\text{g/ml}$  was prepared by dissolving 15 mg of ACV in 10 ml 0.1 N HCl and then 1ml was taken from this sol and diluted to 10 ml with 0.1 N HCl.

The first step was determining the  $\lambda$  max of acyclovir by booking 2 ml of stock solution (150  $\mu\text{g/ml}$ ) in 10 ml volumetric flask and volume was made up to 10 ml with 0.1 N HCl and scanning the solution on UV scanner between 200 to 400 nm and the maxima peak obtained was considered as  $\lambda$  max.

Dilutions set of the drug from the stock solution with known concentrations (2-15 $\mu\text{g/ml}$ ) were organized and analyzed in the spectrophotometer at the wavelength of acyclovir maximum absorbance against blank [17]. By plotting the absorbance reflected against the known concentrations, the calibration curve was obtained.

### 2.2.3 Preparation of Cross-linked Chitosan /Acyclovir granules

100 mg of acyclovir was dissolved in sufficient volume (about 7 ml) of 0.1 N HCl with stirring. One gram of the cross-linked chitosan was placed in a petri dish and adding the acyclovir solution drop by drop

with uniform distribution and continuous mixing until slurry mass was formed.

The slurry was spread over the petri dish area and left to dry at room temperature for 12 hours (hr). Then the mass was passed through a sieve to get the granules and left to dry at room temperature for 6 hours, then in the oven at 50°C for 30 minutes. The granules were put in a closed container for further characterization. The composition of the granules is summarized in Table 1.

## 2.3 Characterization

### 2.3.1 Fourier transform infrared (FT-IR) spectroscopy

FT-IR spectra of chitosan and cross-linked chitosan were recorded on (FTIR-8400S, Shimadzu) instrument using KBr disc in the range of 4000 – 400  $\text{cm}^{-1}$  in order to assess structural changes that could have occurred in the polymer as a result of cross-linking [18].

### 2.3.2 X-ray diffraction measurements (XRD)

The analysis of crystallinity aspects of the acyclovir, pure CS, CLCS, ACV-CLCS physical mix, and ACV loaded-CLCS granules were accomplished with an X-ray diffractometer (Phillips Xpert) that operates at 40 kV, 30 mA using a Copper line focus X-ray tube (Copper anode as X-ray source) with Nickel  $k\beta$  absorber producing  $\text{K}\alpha_1$  radiation ( $\lambda = 1.5406 \text{ \AA}$ ) [19]. Diffraction patterns were recorded over the 2 $\theta$  range of 10–80°.

### 2.3.3 Thermal gravimetric analysis / Differential scanning calorimetry

By using a simultaneous thermal analyzer to measure both heat flow and weight changes in a material as a function of temperature (or time) under a controlled atmosphere, thermal gravimetric analysis (TGA) and differential scanning calorimetry (DSC) of the raw chitosan, CLCS, acyclovir-loaded CLCS granules and physical mixtures were implemented on TA Instrument/SDT Q600 V20.9 Build 20. The samples were heated over a temperature range of 25-700 °C at 20 °C/min heating rate under argon atmosphere [20].

### 2.3.4 Scanning Electron Microscopy (SEM)

The exterior surface and morphological design of the plain CS, CLCS, and acyclovir-loaded CLCS were characterized by field-emission scanning electron-focused microscopy (FESEM). The specimen was spread over a conductive tape, coated with electrically

Table 1. Composition of Acyclovir-loaded crosslinked chitosan granules.

Formula	CLCS weight	Cross-linker Type and amount	Crosslinking percent	Acyclovir weight
FGX1	1 g	Glyoxal 2% 0.217 ml/g of chitosan	3 %	100 mg
FGX2	1 g	Glyoxal 2% 0.435 ml/g of chitosan	6 %	100 mg
FGX3	1 g	Glyoxal 2% 0.87 ml/g of chitosan	12 %	100 mg
FGU1	1 g	Glutaraldehyde 2.5 % 0.3 ml/g of chitosan	3 %	100 mg
FGU2	1 g	Glutaraldehyde 2.5 % 0.6 ml/g of chitosan	6 %	100 mg
FGU3	1 g	Glutaraldehyde 2.5 % 1.2 ml/g of chitosan	12 %	100 mg
FTP1	1 g	Terephthaldehyde 2% 0.5 ml/g of chitosan	3 %	100 mg
FTP2	1 g	Terephthaldehyde 2% 1 ml/g of chitosan	6 %	100 mg
FTP3	1 g	Terephthaldehyde 2% 2 ml/g of chitosan	12 %	100 mg

conducting material (gold) by Sputter coater, scanned and observed by Mira3, Tescan, France [21].

### 2.3.5 Swelling Test

To visualize the swelling behavior of the prepared glyoxal, glutaraldehyde, and terephthaldehyde cross-linked chitosans, a gravimetric procedure was applied [22]. 0.1 g of the CLCS was placed in a simulated dialysis bag (that is secured at both ends) and dipped in a beaker containing 50mL of 0.1 N HCl. The process is conducted at 37°C and 1.2 pH. At determined times, the bags were lifted up and weighing the swelled gel after removing the surplus HCl solution on the surface with filter paper wiping. By evaluating the reflected change in mass, the swelling ratio (S) is assessed using the following equation:  $S \% = (W1 - W0) / W0 \times 100$

where W1 is the weight of the gel after dipping at a particular time and W0 is the weight of initial CLCS powder before immersion.

### 2.3.6 In vitro release study

*In vitro* acyclovir release from acyclovir-loaded CLCS granules was done on the dissolution apparatus USP. Each jar contains 500 ml of freshly prepared 0.1N HCl (pH 1.2) as a dissolution medium in which 1g of each formula (installed within dialysis membrane with 8000-14000 Daltons molecular weight cut-off) was immersed to evaluate the release profile of the drug from the formula. To simulate the gastro-intestinal environment, the apparatus was set at 50 rpm rotation speed and 37 °C under sink condition [23].

Samples of 5ml were picked up at programmed time points from the release medium. The samples were diluted and analyzed at 255 nm with a UV spectrophotometer. After each sampling, replenishment with an equal freshly prepared volume of the dissolution medium was done. In triplicate resumption, the experiments were executed. Then the cumulative percentage of drug release was calculated.

### 2.3.7 Release Kinetics

To investigate the release mechanism of acyclovir from CLCS-ACV formulations, data obtained from *in vitro* drug release analysis were plotted as the cumulative amount of drug release versus time and applied to the best-describing kinetic models including zero-order, first-order, Higuchi's model, and Korsmeyer-Peppas model [24] with equations as follows:

$$\text{-Zero-order: } Q_t = Q_0 + K_0 t,$$

$$\text{-First-order: } \ln(Q_0 - Q_t) = K_1 t,$$

$$\text{-Higuchi: } Q_t = K_H t^{0.5},$$

$$\text{-Korsmeyer-Peppas: } M_t/M_0 = K_p t^n$$

Where  $Q_t$  is the amount of drug released at time  $t$  and  $Q_0$  is the initial amount of drug in the formulation,  $M_t/M_0$  is the fraction of drug released at time  $t$ ,  $K_0$ ,  $K_1$ ,  $K_H$ , and  $K_p$  are zero-order, first-order, Higuchi, and Korsmeyer-Peppas release rate constants, respectively.

$n$  is the release exponent suggestive of the drug release mechanism

$n$  values smaller than 0.5 are described with a Fickian diffusion mechanism,  $0.5 < n < 1$  with non-Fickian

transport (Case II transport), and  $n > 1$  with super case II transport.

The highest coefficient of correlation ( $r^2$ ) was used to decide which model best fits the ACV release pattern [25].

### 3. Results and discussion

#### 3.1 Preparation of crosslinked chitosan (CLCS)

In this study, the CLCS was prepared from the reaction of chitosan and the dialdehydes glyoxal, glutaraldehyde, and terephthaldehyde. The cross-linking process was constructed on the well-known Schiff base condensation reaction on both sides of the dialdehyde involving the carbonyl assembly of the dialdehyde with the amino units of chitosan, with the establishment of an imine (C=N) bond and elimination of water molecules. The reaction involves two monomers of chitosan with one equivalent of the dialdehyde.

To achieve 12 %, 6%, and 3% terephthaldehyde (TP) cross-linked chitosan, the amounts of TP needed to give these products were estimated. Since the cross-linking reaction targeted the free amino moieties of chitosan, so based on the following calculation and by identifying the free  $\text{NH}_2$  proportion of chitosan, the TP quantity was estimated.

By taking one monomer of chitosan with DD 85% that utilized in this work as an assumption, each 167.3 g of chitosan (As molecular weight (MWT) of chitosan = 203 DA + 161 DD where DA represents the degree of acylation and DD degree of diacylation [26]) contains (13.6 g) of free  $\text{NH}_2$  that may react with TP:

<u>Chitosan</u>	<u>free <math>\text{NH}_2</math></u>
167.3 g	13.6 g
1 g	X

So,  $X = 0.081$  g weight (Wt) of free  $\text{NH}_2$  in 1 g of chitosan.

Moles of free  $\text{NH}_2 = \text{Wt} / \text{Mwt of free } \text{NH}_2 = 0.081 \text{ g} / 16 \text{ g/mole} = 0.005 \text{ moles} = 5 \text{ millimoles (mmoles)}$ .

As each one mmole of the aldehyde reacts with two mmoles of chitosan amino groups, so 2.5 mmoles of TP were estimated to be consumed in the crosslinking.

By multiplying the mmoles by the Mwt of TP (134.13 g/mole), the weight of terephthaldehyde was estimated (2.5 mmoles  $\times$  134.13 = 335.32 mg) which represents the amount needed to give 100 % cross-linking of chitosan. Then to achieve 12 %, 6 %, and 3 % cross-linking, 40 mg, 20 mg, and 10 mg of TP were taken respectively for each 1 g of chitosan. By similar calculations, the amount of glutaraldehyde and glyoxal were speculated as in the following Table 2.

Table 2. The estimated amounts in milligrams (mg) of crosslinkers needed to crosslink one gram of chitosan with percentage yield (PE %).

Crosslinker type	Crosslinking percent	Amount (mg)	PE %
Glyoxal	3 %	4.35	81 %
	6 %	8.7	88 %
	12 %	17.4	85 %
Glutaraldehyde	3 %	7.5	83 %
	6 %	15	86 %
	12 %	30	90 %
Terephthaldehyde	3 %	10	91 %
	6 %	20	84 %
	12 %	40	87 %

Photographs of the resulting CLCS products reveal characteristic aspects. For glyoxal crosslinked chitosan, the products showed beige color that increases in intensity to pale brown with increasing crosslinking percent. The color change was more distinct in glutaraldehyde crosslinked chitosan as shown in Figure 2. In 3% glutaraldehyde CLCS, the color was brown that became darker with increasing crosslinker ratio. Terephthaldehyde crosslinked chitosan color was light brown and shows change with increasing crosslinker amount. The product yield percentage (%) of cross-linked chitosan derivatives is listed in Table 2.

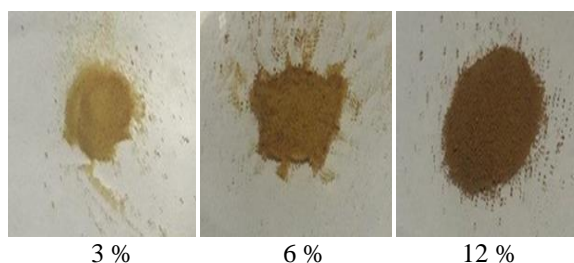


Fig. 2. Photographs of Glutaraldehyde-crosslinked chitosan with increasing crosslinking ratio.

The postulated mechanism for the reaction of chitosan with the dialdehydes (Schiff base reaction) initiates via nucleophilic attack by the nitrogen of the chitosan amino group on the carbonyl of the dialdehyde forming an intermediate of carbonylamine. Dehydration of carbonylamine establishes a carbon-nitrogen double bond (an imine) for glutaraldehyde [27].

#### 3.2 Identification of Acyclovir

##### -Melting point

The melting point of ACV powder was found to be (255°C) which indicates the purity of the acyclovir

used as the melting point was sharp and within the reported standard range [28].

#### -Calibration curve

The maximum absorbance of acyclovir was recorded at (255 nm) wavelength in 0.1N HCl which is close to the reported one [28]. The calibration curve of Acyclovir in 0.1N HCl was estimated with aliquots ranging from (2-15  $\mu\text{g/ml}$ ) at the wavelength of maximum absorbance (255 nm) with a linear correlation coefficient of ( $R^2 = 0.9998$ ).

### 3.3 Characterization

#### 3.3.1 Fourier transform infrared (FT-IR) spectroscopy

According to the spectrum obtained in Figure 3, the broad band at the range of  $3400\text{ cm}^{-1}$  was attributed to the stretching vibration of O-H and N-H. Bands attributed to C-H stretching vibration was identified at about  $2927$  and  $2889\text{ cm}^{-1}$ . Peaks at  $1657\text{ cm}^{-1}$  (vibration modes of amide I),  $1583\text{ cm}^{-1}$  ( $\text{NH}_2$  bending vibration in the amino group)  $1479$  and  $1379\text{ cm}^{-1}$  (bending vibration of  $\text{CH}_3$  and  $\text{CH}_2$  in the ring) were also reported in the IR spectrum of chitosan. The bands at about  $1153\text{ cm}^{-1}$ ,  $1072\text{ cm}^{-1}$  and  $1031\text{ cm}^{-1}$  were specified for C-O-C bridge and C-O stretching vibrations. The  $\beta$ -(1,4) glycosidic bond absorption peak was defined at  $898\text{ cm}^{-1}$ . The out-of-plane bending -OH vibrations are detected at  $653\text{ cm}^{-1}$ .

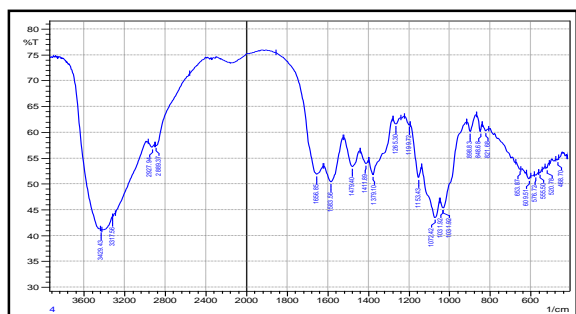


Fig. 3. FT-IR Spectrum of Chitosan.

For the crosslinked chitosan, the new sharp peak at about  $1610\text{ cm}^{-1}$  represents stretching vibrations of  $\text{C}=\text{N}$  in Schiff's base formed by the reaction of the aldehyde and chitosan as observed in Figure 4 where A represents IR spectrum for glyoxal-crosslinked chitosan, B for glutaraldehyde-crosslinked, and C for terephthaldehyde-crosslinked chitosan. Closely related FT-IR results were also obtained for glutaraldehyde-crosslinked chitosan prepared by Ramachandran *et al* [29].

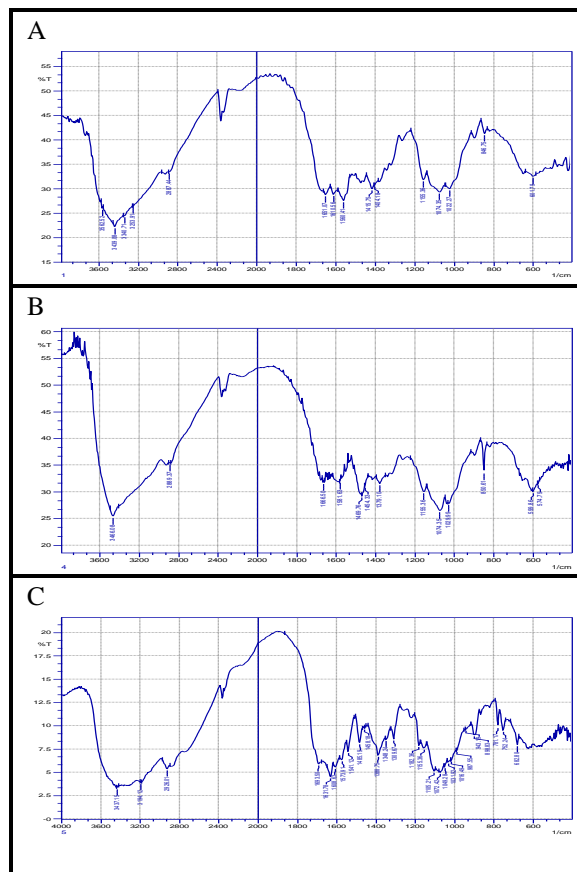


Fig. 4. FT-IR Spectrum of cross-linked chitosan.

#### 3.3.2 X-Ray Diffraction (XRD)

The XRD spectra of chitosan and crosslinked chitosan are shown in Figure 5. Chitosan XRD exhibits a semi crystalline peak at about  $2\theta$  of  $19.8^\circ$  which is attributed to intermolecular and intramolecular hydrogen bindings formed between amino groups and hydroxyl parts that impart crystalline arrangement to chitosan. This result was agreed with the findings of Baran *et al* who characterized chitosan by XRD that showed a strong peak at  $2\theta$  of  $19.68^\circ$  [30].

On the other hand, crosslinked chitosan XRD spectra showed broader shifted peaks with decreased intensity in compared to free chitosan because of distortion of several inter-molecular and intramolecular hydrogen bonding as a set of amino groups are involved in crosslinking. Results also revealed that with increasing the percent of crosslinking, the peak becomes broader and weaker in intensity. In 12 % glyoxal crosslinked chitosan, the broader peak is shifted to about  $21.2^\circ$ , in 12 % glutaraldehyde crosslinked chitosan appears near  $20.7^\circ$ , and in 12 % terephthaldehyde crosslinked one, the peak is found at about  $20.6^\circ$  compared to chitosan.

These results suggest that crosslinked chitosan derivatives have more amorphous and less crystalline

structure than the basic chitosan, which is consistent with previous similar conclusions of Baran [31], Gao *et al* [32] and Demetgül and Beyazit [33] who prepared variant crosslinked chitosans that revealed decreased-intensity and broader peak compared to CS on XRD pattern.

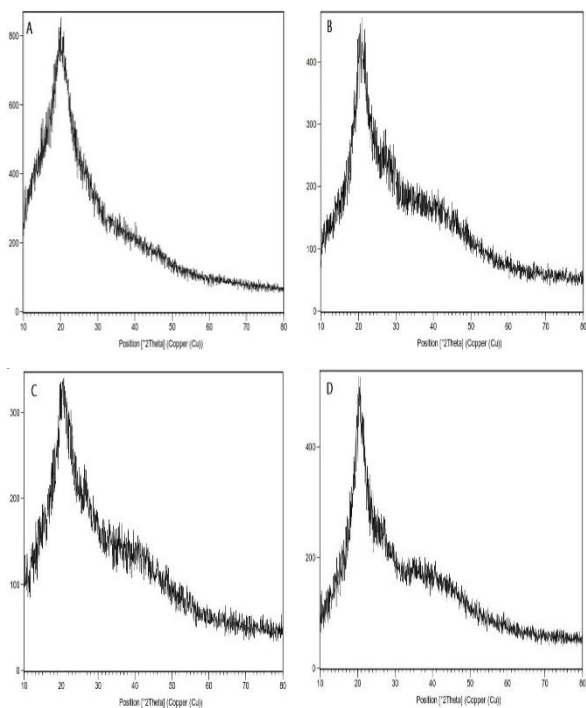


Fig. 5. XRD of A) Chitosan B) Glyoxal crosslinked chitosan C) Glutaraldehyde crosslinked chitosan and D) Terephthalaldehyde crosslinked chitosan.

To predict if there is any chemical interaction between acyclovir and crosslinked chitosan or change in crystallinity when they are incorporated, XRD for pure drug ACV, ACV-CLCS formulas and their physical mix was performed. XRD of ACV (Figure 6) revealed sharp peaks indicating the crystalline structure of acyclovir.

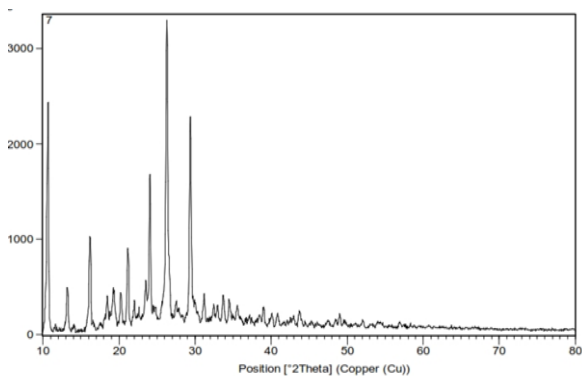
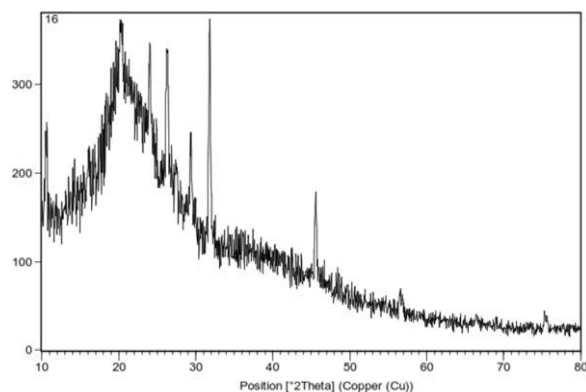
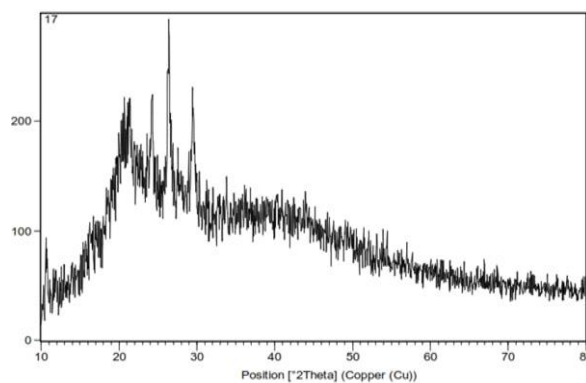


Fig. 6. XRD of Acyclovir

Regarding ACV-CLCS formulas and physical mixtures, all the formulas and their physical blends showed the broad shifted peak of crosslinked chitosan along with the characteristic crystalline peaks of acyclovir (Figure 7). XRD was also used for the identification of the crystalline form of the drug (anti-HIV drug UC 781) after dispersion with Eudragit by Goddeeris *et al* [34]. These results emphasize that there is no chemical consolidation between ACV and CLCS in the current work.



(A)



(B)

Fig. 7. XRD of (A) Glyoxal crosslinked chitosan-acyclovir formula and (B) Glyoxal crosslinked chitosan-acyclovir physical mix.

### 3.3.3 Thermal gravimetric analysis (TGA) and differential scanning calorimetry (DSC)

The thermal properties of chitosan and crosslinked chitosan were examined depending on TGA and DSC methods. For pure chitosan as shown in Figure 8, weight loss took place in two stages. The first one arises at 60-105 °C with a weight loss of 10% which may be correlated to the loss of water. The second stage starts at 250 °C with a maximum at 350 °C with a weight loss of 45 % and continued to the end of the TGA which corresponds to the decomposition of chitosan, splitting of glycosidic bonds and the decomposition of the glucosamine units.

The DSC of chitosan displays an endothermic peak around 100°C that may be specified for the loss of water associated with the chitosan hydrophilic groups and an exothermic peak at about 328°C that may assign to the thermal decomposition of chitosan. Close results of chitosan TGA and DSC were identified by Al-Amin *et al* that revealed comparable weight loss stages and peaks [35].

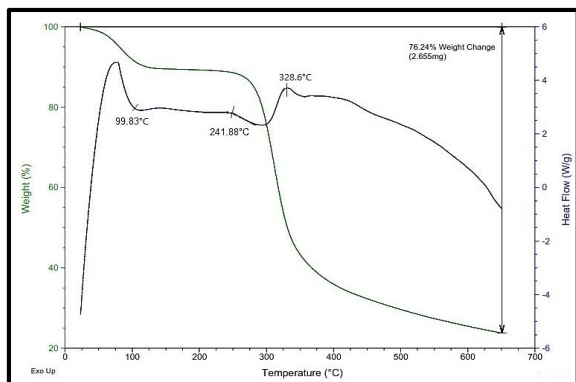


Fig. 8. TGA and DSC of chitosan.

For glyoxal-crosslinked chitosan (Figure 9), the TGA shows two stages of weight loss distinct from that of chitosan: the first stage between 50-140°C representing water loss phase that occurs at a wider range and shifted to a higher peak than that of chitosan because of chain crosslinking hindrance of moisture removal, the second stage starts at 230-700°C that may match the phase of the splitting of cross-linkages, random glycosidic bonds cleavage and chitosan backbone degradation. Datta *et al* also obtained comparative results that glyoxal-crosslinked chitosan needs higher temperature than chitosan to lose the tightly bounded water at a range that reached 156°C [36].

The DSC thermograms revealed an endothermic peak above 100°C with a different area and position from that of chitosan which corresponds to the temperature of water removal confirming the previous finding in TGA as chitosan and crosslinked chitosan differ in their water-holding capacity. The DSC reflects significant change when increasing the percent of crosslinking as 3 % glyoxal crosslinked chitosan exhibits an endothermic peak at about 104 °C which is shifted to 119.9 °C in 12 % crosslinked one that means more hindrance of water removal because of stronger interaction that requires a higher temperature to remove this water. Another significant change, DSC also manifests an exothermic peak at about 283°C in 3 % that is shifted to 295 °C in 12 % one that corresponds to the temperature of glyoxal crosslinked chitosan decomposition demonstrating that 12 % crosslinked is more stable than 3 % cross-linked chitosan.

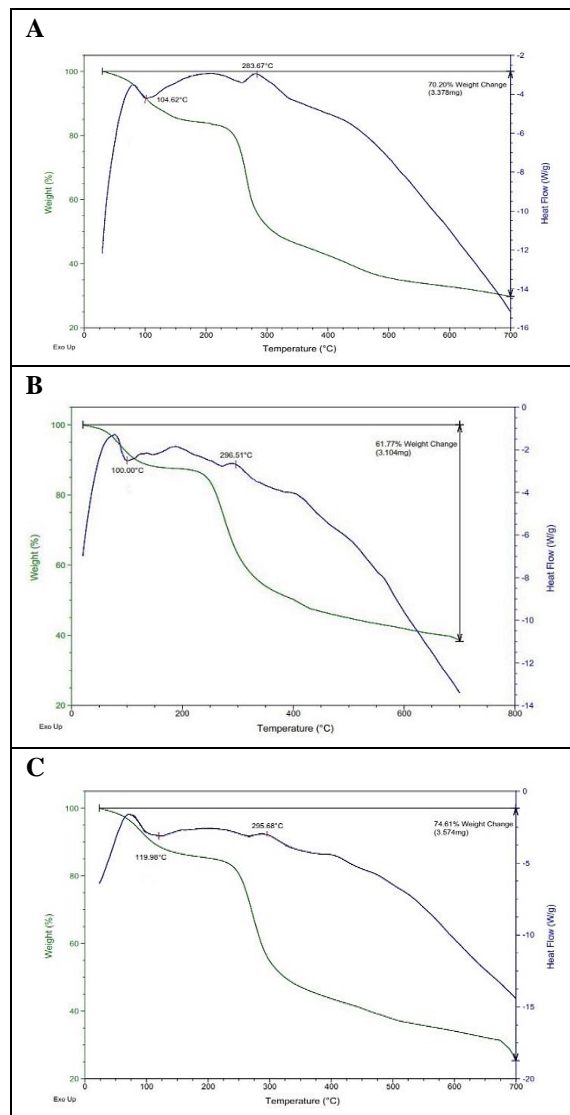


Fig. 9. TGA and DSC of glyoxal-crosslinked chitosan: A: 3 % crosslinking B: 6 % crosslinking and C: 12 % crosslinking.

For glutaraldehyde crosslinked chitosan (Figure 10), TGA also shows two stages of weight loss: the first as in glyoxal crosslinked chitosan with a wider range than chitosan between 50-150 °C which corresponds to the water removal indicating the bounded water in crosslinked chitosan is more difficult to remove than in parent chitosan and the second stage stands for cleavage of cross linkages and chitosan monomers degradation at range 235-700°C.

The DSC of glutaraldehyde crosslinked chitosan also elucidates change in position and area of the endothermic peak (that corresponds to the water removal) with increasing the crosslinking ratio. The peak is weak in 3 % crosslinked while it is apparent at about 104°C in 12 % crosslinked chitosan reflecting that

bounded water removal from 12% crosslinked is more difficult than 3 % crosslinked chitosan. The DSC reveals an exothermic peak above 300°C that may be marked for crosslinking incision and thermal decomposition. Neto *et al* thermally analyzed chitosan and glutaraldehyde crosslinked chitosan and revealed similar results that there are differences in their water-polymer interaction and moisture-holding capacity [37].

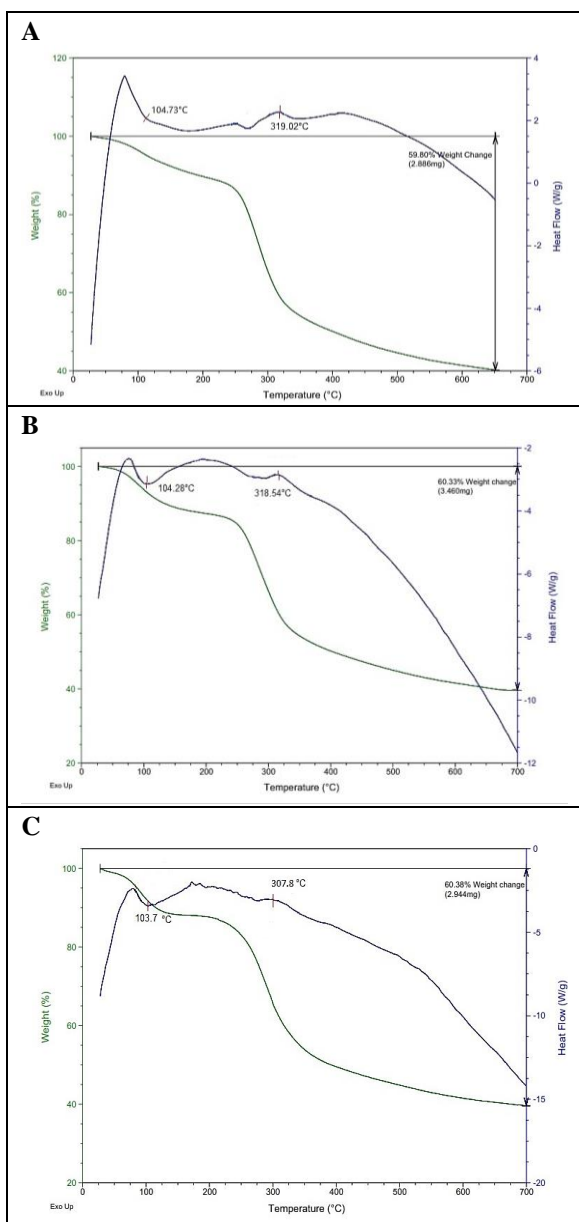


Fig. 10. TGA and DSC of glutaraldehyde-crosslinked chitosan: A: 3 % crosslinking B: 6 % crosslinking and C: 12 % crosslinking.

For terephthaldehyde crosslinked chitosan, the thermal analysis (Figure 11) manifests two steps of weight loss. The first one runs at 60°C and extends

till 180°C representing the water removal stage which occurs at a higher temperature than chitosan because the bounded water has a stronger interaction with crosslinked chitosan as crosslinking forms spaces that can hold water molecules restricting its removal. The second step happens at 230-700°C signifying the decomposition stage of terephthaldehyde crosslinked chitosan.

The DSC of terephthaldehyde crosslinked chitosan exhibits an endothermic peak at 109°C in 3 % crosslinked that is shifted to 111.75°C in 12 % crosslinked which is attributed to the loss of water. The DSC also reveals an exothermic peak around 300°C in all percent of crosslinking which states for thermal decomposition of the crosslinked chitosan. Comparable thermal results for chitosan and terephthaldehyde crosslinked chitosan were also exposed by Santosh and Joonseok [38].

As a summary, crosslinked chitosan compared to raw chitosan reveals different water-holding capacities. In chitosan, water molecules can be bound to two polar groups, hydroxyl and more predominantly to the amine groups. Cross-linked chitosan has less amino groups available to form hydrogen bonds with water molecules. Consequently, most of the water molecules will be bound to chitosan hydroxyl groups by hydrogen bonds which are stronger than the ones with the amino groups which explains why a higher temperature would be required to remove such water molecules [37].

Near the end of the TGA experiment at 650°C, the residual amount of chitosan is only 23% while for all crosslinked chitosan the residual amount is around 40 %. From these results, it is evident that crosslinked chitosan has more thermal stability compared to uncrosslinked chitosan. Similar findings were identified by Aisverya *et al* work in which thermogravimetric analysis signified that the thermal stability of chitosan was increased with glutaraldehyde using as a crosslinking agent [39].

DSC and TGA were also done for the crosslinked chitosan-acyclovir formulations and their physical mixtures to exclude any chemical interactions between acyclovir and crosslinked chitosan. Thermograms (Figure 12) display the characteristic peaks of crosslinked chitosan mentioned above with a poorly defined endothermic peak around 260°C that is aligned with the acyclovir melting. The reason for this poor appearance may be due to the small amount of acyclovir incorporated within the formulation or the fast heating rate [40].

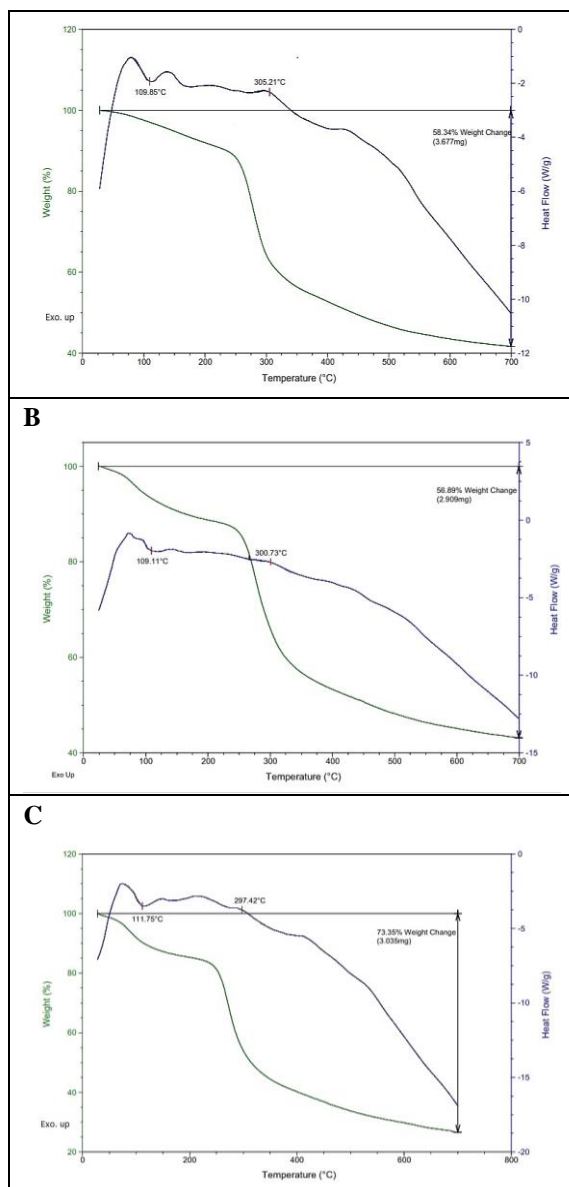


Fig. 11. TGA and DSC of terephthaldehyde-crosslinked chitosan: A: 3 % crosslinking B: 6 % crosslinking and C: 12 % crosslinking.

### 3.3.4 Scanning electron microscopy (SEM)

Untreated chitosan and crosslinked derivatives were investigated by means of SEM (Figure 13). The chitosan image reveals a smooth and flat surface while the SEM of CLCS demonstrates areas with rough surfaces with grooves and wrinkles. These observations were in line with Hassan *et al* work when chitosan Schiff base derivatives revealed increase surface roughness compared to raw chitosan [41] and Bin Li *et al* investigation that showed rough-surface glutaraldehyde cross-linked chitosan [42]. The reported wrinkles may be preferable sites for drug deposition and holding.

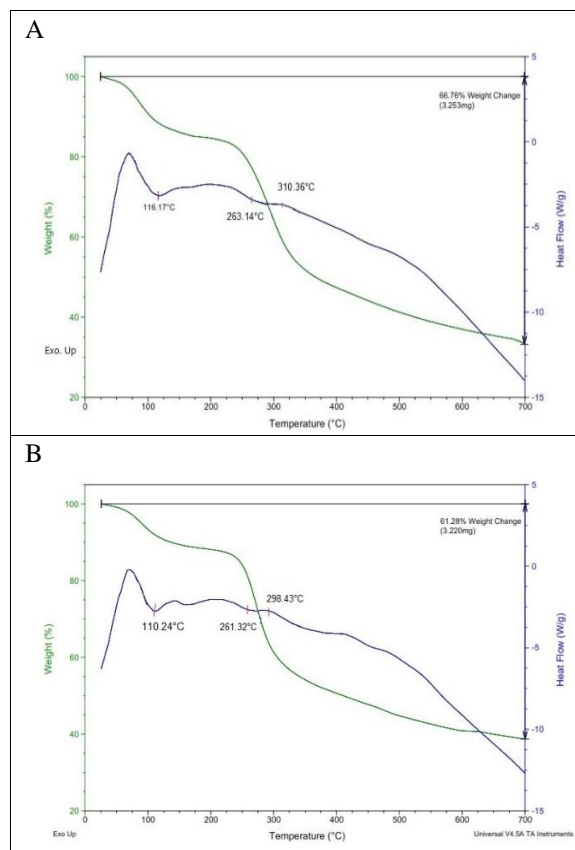


Fig. 12. DSC and TGA of A) 12% glyoxal cross-linked chitosan acyclovir formulation B) 12% glyoxal cross-linked chitosan acyclovir physical mix.

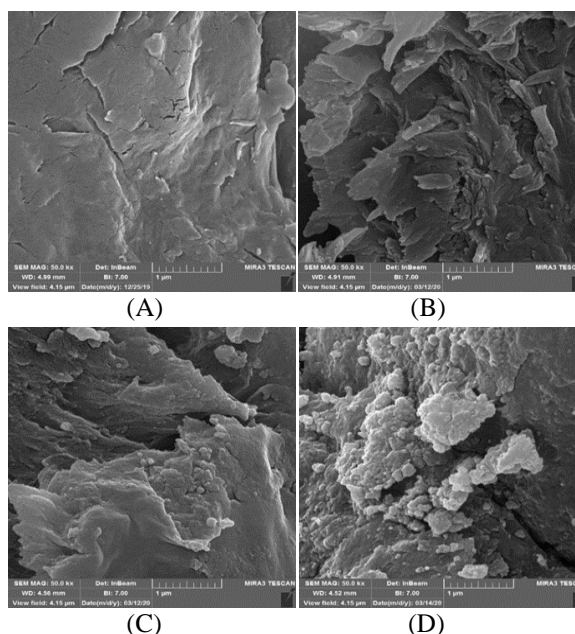


Fig. 13. SEM of A) Chitosan B) 6 % Glyoxal crosslinked chitosan C) 12 % Glutaraldehyde crosslinked chitosan D) 6 % Terephthaldehyde crosslinked chitosan.

SEM also reflects the effect of crosslinking amount on chitosan surface morphology (Figure 14). Increasing the percent of crosslinking produces chitosan with more compact, denser, smoother, and less porous than chitosan with a lower crosslinker percent. So, when acyclovir is incorporated with CLCS, the denser surface with fewer pores (for CS with higher crosslinker percent) may produce more control of the drug release. These observations were consistent with Raman *et al* conclusion in polyacrylamide hydrogels synthesis that a higher amount of crosslinker produced smoother surfaces with lesser pores [43].

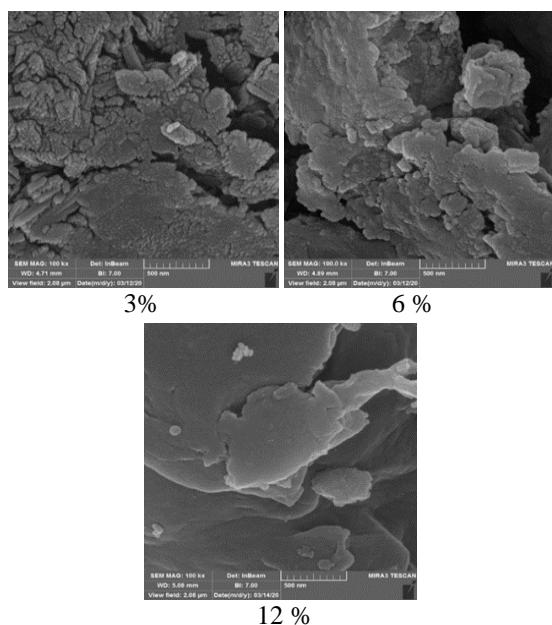


Fig. 14. SEM of Glyoxal crosslinked chitosan with three different percent of crosslinking.

SEM for crosslinked chitosan-acyclovir granules (Figure 15) displays acyclovir embedded in crosslinked chitosan matrix indicating good compatibility between the CLCS and the drug. Acyclovir particles became more obvious under higher magnification as revealed in Figure 15 (B).

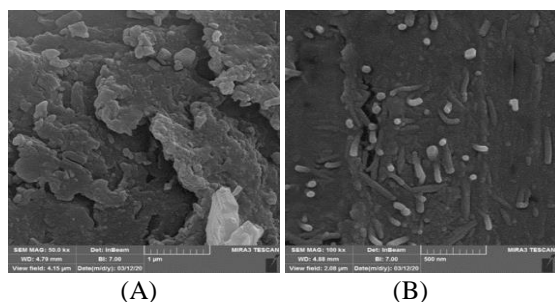
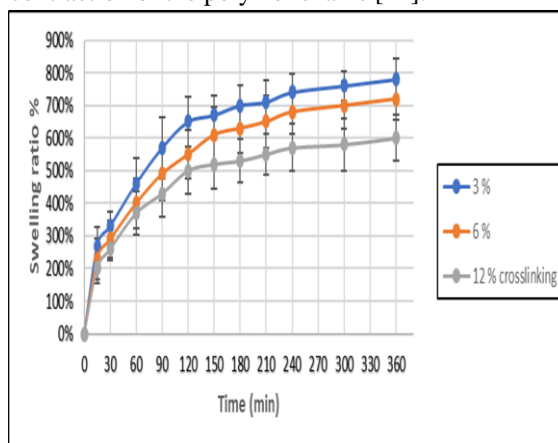


Fig. 15. SEM for crosslinked chitosan-acyclovir granules: (A) Glyoxal crosslinked (B) Glutaraldehyde crosslinked.

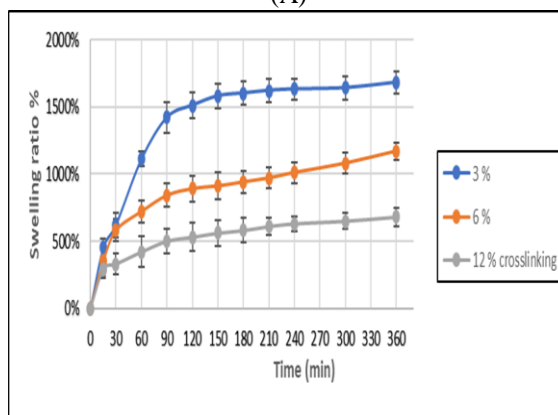
### 3.3.5 Swelling test

Chitosan as a porous polymer inclines to absorb water molecules and expands in acidic conditions because of the presence of N-H<sub>2</sub> and O-H functional groups. The (-NH<sub>2</sub>) functional groups were considerably protonated in acidic solution into (-NH<sub>3</sub><sup>+</sup>) cations on the chitosan chains inducing electrostatic repulsion between charged monomers conferring increment in the space among these chains. The higher space between chitosan chains might increase the penetration of water within the polymer [22].

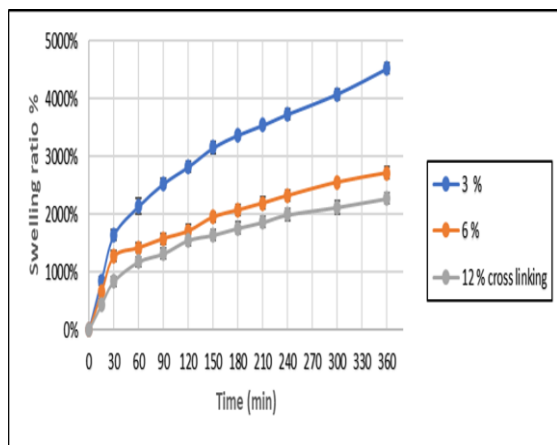
The crosslinked chitosan displayed less swelling, and the degree of swelling was revealed to decrease with increasing the density of crosslinking agent (Figure 16). The proper justification is as the crosslinking agent percent increases, more amine units of chitosan are exhausted in the crosslinking interactions, so the crosslinked chitosan turns less qualified for hydrogen bonding with water molecules with movability restriction and contraction of the polymer chains [44].



(A)



(B)



(C)

Fig. 16. Swelling behavior of (A) Glyoxal crosslinked chitosan (B) Glutaraldehyde crosslinked chitosan and (C) Terephthaldehyde crosslinked chitosan (n=3).

As chitosan is a swellable polymer, when incorporated with a drug, the release of the drug is controlled by the degree of swelling. The high porosity of chitosan might be responsible for the rapid release of the drug. Increasing the percent of chitosan crosslinking from 3 % to 12 % leads to less swellable polymer and so may produce slower drug release.

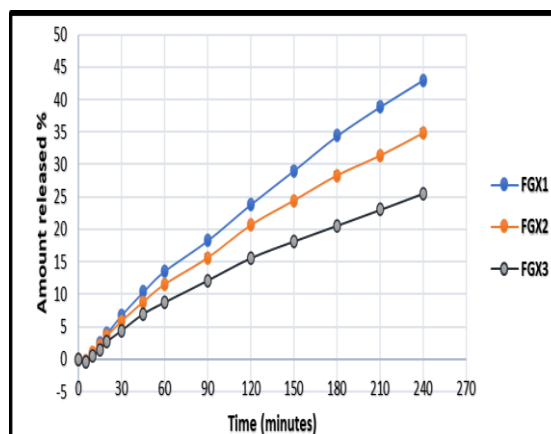
### 3.3.6 In vitro drug release

The drug (acyclovir) release data from the CLCS-ACV granules are shown in Figure 17. Results displayed that acyclovir release demonstrated a biphasic release pattern with initial burst release might be due to the diffusion of the drug from the surface of the formulation and subsequent sustained release phenomenon governed by swelling of the polymeric matrix and diffusion of the entrapped acyclovir.

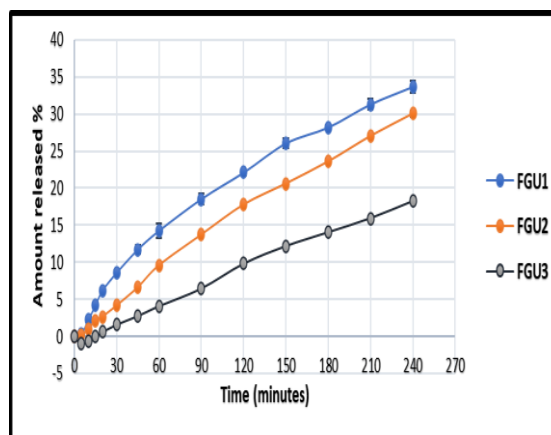
The cumulative amount of acyclovir release was established to be driven by the type and concentration of the cross-linking agent. For instance, glyoxal-chitosan-acyclovir granules (FGX) exhibited a higher percent of drug release when compared to glutaraldehyde-chitosan-acyclovir (FGU) or terephthaldehyde-chitosan-acyclovir (FTP) granules. This indicated that the matrix formed between chitosan-glutaraldehyde and chitosan-terephthaldehyde is less flexible than the chitosan-glyoxal and hence affected the drug release rate.

Furthermore, increase the percent of the crosslinker led to a slower drug release rate. This is because increasing the crosslinker concentration

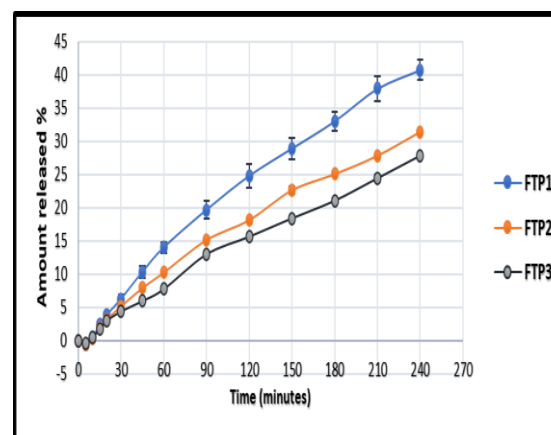
generates less-swellable highly crosslinked chitosan with reduced diffusion pathways.



(A)



(B)



(C)

Fig. 17. Acyclovir release from: A) glyoxal crosslinked chitosan-acyclovir granules (FGX) B) glutaraldehyde crosslinked chitosan-acyclovir granules (FGU) C) terephthaldehyde crosslinked chitosan-acyclovir granules (FTP) (n=3).

In conclusion, crosslinking of chitosan modifies its drug-holding capacity resulting in controlling the release of acyclovir. The sustained release of acyclovir can enhance the oral bioavailability of ACV, reduce the frequency of dosing, and so may result in better patient compliance [45].

### 3.3.7 Release kinetics

The *In vitro* release profile was applied on various kinetic models (zero, first, Higuchi, and Korsmeyer-Peppas) in order to find out the mechanism of drug release. Table 3 shows the correlation coefficients and rate constants obtained. From the results gained with considering the kinetic model with the highest  $r^2$  values, it could be emphasized that acyclovir release from CLCS-ACV formulations obeys first-order kinetics ( $r^2$  around 0.99 for all formulations with one formula with 0.979), indicating the ACV release is concentration-dependent.

It was also observed that ACV release demonstrates a high correlation with Higuchi model ( $r^2$  around 0.936-0.988 for all formulations) which elucidates that the ACV release from CLCS-ACV formulations is controlled by diffusion.

The *in vitro*-release data obtained was also fitted to Korsmeyer-Peppas equation to confirm whether the ACV release mechanism is Fickian diffusion, non-Fickian diffusion, or zero-order. Good fitting was noted with exponent ( $n$ ) values higher than 1 for almost all formulations suggesting super case II transport as the major release mechanism confirming acyclovir release is governed by polymer relaxation (swelling).

To sum up, the swelling and diffusion release mechanisms may coincide in control the ACV release from the CLCS-ACV granules [46].

Table 3: The rate constants and correlation coefficients of the model equations of the *in vitro* release kinetics.

Formula	Zero-order		First-order		Higuchi		Korsmeyer-Peppas		
	$k_0$	$r^2$	$k_1$	$r^2$	$k_H$	$r^2$	$k_P$	$r^2$	$n$
<b>FGX1</b>	0.1852	0.9932	0.0024	<b>0.9989</b>	0.0305	0.9757	0.0012	0.96	1.106
<b>FGX2</b>	0.1502	0.9887	0.0018	<b>0.9969</b>	0.0248	0.9689	0.0015	0.9775	1.026
<b>FGX3</b>	0.1106	0.9824	0.0013	<b>0.9907</b>	0.0184	0.9724	0.0008	0.9435	1.101
<b>FGU1</b>	0.1415	0.9618	0.0017	0.9792	0.024	<b>0.988</b>	0.0021	0.9087	0.983
<b>FGU2</b>	0.1294	0.9914	0.0015	<b>0.9972</b>	0.0213	0.9631	0.0004	0.9302	1.251
<b>FGU3</b>	0.082	0.9944	0.0009	<b>0.9961</b>	0.0133	0.936	0.0002	0.9813	1.291
<b>FTP1</b>	0.1796	0.9843	0.0023	<b>0.9959</b>	0.0298	0.9689	0.0008	0.923	1.193
<b>FTP2</b>	0.1359	0.9842	0.0016	<b>0.9932</b>	0.0225	0.9695	0.0006	0.9124	1.181
<b>FTP3</b>	0.1178	0.9911	0.0014	<b>0.9959</b>	0.0194	0.9615	0.0008	0.9486	1.098

## 4. Conclusions

Crosslinked chitosan derivatives were successfully prepared from the Schiff base condensation reaction of chitosan and the dialdehydes glyoxal, glutaraldehyde, and terephthaldehyde with the establishment of an imine (C=N) bond as evidenced in FTIR. The crosslinking was done in three different ratios for each dialdehyde, showing an obvious difference in the modulation of chitosan properties as revealed by

XRD, DSC, TGA, SEM, swelling ratio, and thereby the drug-release properties.

Results displayed that acyclovir release demonstrated a biphasic release pattern with initial burst release might be due to the diffusion of the drug from the surface of the formulation and subsequent sustained release phenomenon governed by swelling of the polymeric matrix and diffusion of the entrapped acyclovir and increasing the percent of the crosslinker led to slower drug release rate. This sustained release

of acyclovir can enhance the oral bioavailability of ACV, reduce the frequency of dosing, and so result in better patient compliance.

### 5. Conflicts of interest

There are no conflicts to declare.

### 6. Acknowledgments

The researchers are thankful to the pharmaceutical chemistry and pharmaceuticals Departments, College of Pharmacy, University of Basra, Iraq (director and members) for their support during the course of this study.

### 7. References

- [1] Thakur V.K., Thakur M.K., Recent advances in graft copolymerization and applications of chitosan: a review, *ACS Sustainable Chemistry and Engineering* 2(12) (2014) 2637-2652.
- [2] Ahmed A.S., Hassan A.M., Nour M.H., Utilization of Chitosan Extracted from Shrimp Shell Waste in Wastewater Treatment as Low Cost Biosorbent, *Egyptian Journal of Chemistry* 64(2) (2021) 981-988.
- [3] Berezina N., Production and application of chitin, *Physical Sciences Reviews* 1(9) (2016) 1-8.
- [4] Souza C.P., Almeida B.C., Colwell R.R., Rivera I.N.G., The Importance of Chitin in the Marine Environment, *Marine Biotechnology* 13(5) (2011) 823-830.
- [5] Rouget C., Des substances amylicées dans les tissus des animaux, spécialement des Articulés (chitine), *Comptes Rendus* 48 (1859) 792-795.
- [6] Mohebbi S., Nezhad M.N., Zarrintaj P., Jafari S.H., Gholizadeh S.S., Saeb M.R., Mozafari M., Chitosan in biomedical engineering: a critical review, *Current Stem Cell Research and Therapy* 14(2) (2019) 93-116.
- [7] Ahmed S., Ikram S., Chitosan & its derivatives: A review in recent innovations, *International Journal of Pharmaceutical Sciences and Research* 6(1) (2015) 14-30.
- [8] Younes I., Rinaudo M., Chitin and chitosan preparation from marine sources. Structure, properties and applications, *Marine Drugs* 13(3) (2015) 1133-1174.
- [9] Abraham S., Rajamanickam D., Srinivasan B., Preparation, characterization and cross-linking of chitosan by microwave assisted synthesis, *Science International* 6(1) (2018) 18-30.
- [10] Shukla S.K., Mishra A.K., Arotiba O.A., Mamba B.B., Chitosan-based nanomaterials: A state-of-the-art review, *International Journal of Biological Macromolecules* 59 (2013) 46-58.
- [11] Kim S., Competitive Biological Activities of Chitosan and Its Derivatives: Antimicrobial, Antioxidant, Anticancer, and Anti-Inflammatory Activities, *International Journal of Polymer Science* 2018 (2018) 1-13.
- [12] Kamburov M., Simeonova M., Daunorubicin-loaded chitosan microparticles-preparation and physicochemical characterization, *Journal of Chemical Technology and Metallurgy* 51(1) (2016) 39-46.
- [13] Beppu M.M., Vieira R.S., Aimoli C.G., Santana C.C., Crosslinking of chitosan membranes using glutaraldehyde: Effect on ion permeability and water absorption, *Journal of Membrane Science* 301(1) (2007) 126-130.
- [14] Bruni G., Maietta M., Maggi L., Mustarelli P., Ferrara C., Berbenni V., Milanese C., Girella A., Marini A., Preparation and Physicochemical Characterization of Acyclovir Cocrystals with Improved Dissolution Properties, *Journal of Pharmaceutical Sciences* 102(11) (2013) 4079-4086.
- [15] Pavani S., Mounika K., Naresh K., Formulation and Evaluation of Acyclovir Microspheres, *Iraqi Journal of Pharmaceutical Sciences* 27(1) (2018) 1-7.
- [16] Al-Abadi A.N., Rassol A.A.A., Preparation and in-vitro evaluation of floating microspheres of gabapentin, *Kufa Journal for Veterinary Medical Sciences* 2(1) (2011) 77-92.
- [17] Preeti G., Momin N., Kharade S., Konapure N., Kuchekar B., Spectrophotometric estimation of acyclovir in pharmaceutical dosage forms, *Indian Journal of Pharmaceutical Sciences* 68(4) (2006) 516-517.
- [18] Kumari S., Kumar Annamareddy S.H., Abanti S., Kumar Rath P., Physicochemical properties and characterization of chitosan synthesized from fish scales, crab and shrimp shells, *International Journal of Biological Macromolecules* 104 (2017) 1697-1705.
- [19] Pavoni J.M.F., dos Santos N.Z., May I.C., Pollo L.D., Tessaro I.C., Impact of acid type and glutaraldehyde crosslinking in the physicochemical and mechanical properties and biodegradability of chitosan films, *Polymer Bulletin* 78(2) (2021) 981-1000.
- [20] Hafeez S., Islam A., Gull N., Ali A., Khan S.M., Zia S., Anwar K., Khan S.U., Jamil T.,  $\gamma$ -Irradiated chitosan based injectable hydrogels for controlled release of drug (Montelukast sodium), *International Journal of Biological Macromolecules* 114 (2018) 890-897.
- [21] Zahir A., Aslam Z., Kamal M.S., Ahmad W., Abbas A., Shawabkeh R.A., Development of novel cross-linked chitosan for the removal of anionic Congo red dye, *Journal of Molecular Liquids* 244 (2017) 211-218.
- [22] Darbasizadeh B., Motasadizadeh H., Foroughi-Nia B., Farhadnejad H., Tripolyphosphate-crosslinked chitosan/poly (ethylene oxide) electrospun nanofibrous mats as a floating gastro-retentive delivery system for ranitidine hydrochloride, *Journal of Pharmaceutical Biomedical Analysis* 153 (2018) 63-75.
- [23] Ahmad U., Sohail M., Ahmad M., Minhas M.U., Khan S., Hussain Z., Kousar M., Mohsin S., Abbasi M., Shah S.A., Chitosan based thermosensitive injectable hydrogels for controlled delivery of loxoprofen: development, characterization and in-vivo evaluation, *International Journal of Biological Macromolecules* 129 (2019) 233-245.
- [24] Singhvi G., Singh M., In-vitro drug release characterization models, *International Journal of Pharmaceutical Studies and Research* 2(1) (2011) 77-84.
- [25] Nayak U.Y., Gopal S., Mutalik S., Ranjith A.K., Reddy M.S., Gupta P., Udupa N., Glutaraldehyde cross-linked chitosan microspheres for controlled delivery of zidovudine, *Journal of microencapsulation* 26(3) (2009) 214-222.
- [26] Zhang H., Li Y., Zhang X., Liu B., Zhao H., Chen D., Directly determining the molecular weight of chitosan

- with atomic force microscopy, *Frontiers Nanoscience Nanotechnology* 2(3) (2016) 123-127.
- [27] Akakuru O., Isiuku B., Chitosan hydrogels and their glutaraldehyde-crosslinked counterparts as potential drug release and tissue engineering systems-synthesis, characterization, swelling kinetics and mechanism, *Journal of Physical Chemistry & Biophysics* 7(3) (2017) 1-7.
- [28] Moffat A.C., Osselton M.D., Widdop B., Watts J., Clarke's analysis of drugs and poisons, 4th ed., Pharmaceutical press, London 2011.
- [29] Ramachandran S., Nandhakumar S., Dhanaraju M.D., Formulation and characterization of glutaraldehyde cross-linked chitosan biodegradable microspheres loaded with famotidine, *Tropical Journal of Pharmaceutical Research* 10(3) (2011) 309-316.
- [30] Baran T., Açıksöz E., Menteş A., Highly efficient, quick and green synthesis of biarilys with chitosan supported catalyst using microwave irradiation in the absence of solvent, *Carbohydrate Polymers* 142 (2016) 189-198.
- [31] Baran T., New Chitosan-Glyoxal Beads Supported Pd (II) Catalyst: Synthesis, Characterization and Application in Suzuki Coupling Reactions, *Haceteppe Journal of Biology and Chemistry* 44(3) (2016) 307-315.
- [32] Gao H., Zhou W., Jang J.-H., Goodenough J.B., Cross-Linked Chitosan as a Polymer Network Binder for an Antimony Anode in Sodium-Ion Batteries, *Advanced Energy Materials* 6(6) (2016) 1-7.
- [33] Demetgül C., Beyazit N., Synthesis, characterization and antioxidant activity of chitosan-chromone derivatives, *Carbohydrate Polymers* 181 (2018) 812-817.
- [34] Goddeeris C., Willems T., Houthoofd K., Martens J.A., Van den Mooter G., Dissolution enhancement of the anti-HIV drug UC 781 by formulation in a ternary solid dispersion with TPGS 1000 and Eudragit E100, *European Journal of Pharmaceutics and Biopharmaceutics* 70(3) (2008) 861-868.
- [35] Dey S.C., Al-Amin M., Rashid T.U., Sultan M., Ashaduzzaman M., Sarker M., Shamsuddin S., Preparation, characterization and performance evaluation of chitosan as an adsorbent for remazol red, *International Journal of Latest Research in Engineering and Technology* 2(2) (2016) 52-62.
- [36] Maity S., Datta A., Lahiri S., Ganguly J., Selective separation of 152 Eu from a mixture of 152 Eu and 137 Cs using a chitosan based hydrogel, *RSC Advances* 5(109) (2015) 89338-89345.
- [37] Neto C.d.T., Giacometti J.A., Job A.E., Ferreira F.C., Fonseca J.L.C., Pereira M.R., Thermal analysis of chitosan based networks, *Carbohydrate Polymers* 62(2) (2005) 97-103.
- [38] Kumar S., Koh J., Physicochemical and optical study of chitosan-terephthaldehyde derivative for biomedical applications, *International journal of biological macromolecules* 51(5) (2012) 1167-1172.
- [39] Aisverya S., Sangeetha K., Venkatesan J., Gomathi T., Sudha P., Preparation and Characterization of Chitosan-Povidone Blend with Glutaraldehyde as Crosslinking agent, *World Journal of Pharmaceutical Research* 7(5) (2018) 1926-1940.
- [40] Bikiaris D., Papageorgiou G.Z., Stergiou A., Pavlidou E., Karavas E., Kanaze F., Georgarakis M., Physicochemical studies on solid dispersions of poorly water-soluble drugs: Evaluation of capabilities and limitations of thermal analysis techniques, *Thermochimica Acta* 439(1) (2005) 58-67.
- [41] Hassan M.A., Omer A.M., Abbas E., Baset W.M.A., Tamer T.M., Preparation, physicochemical characterization and antimicrobial activities of novel two phenolic chitosan Schiff base derivatives, *Scientific Reports* 8(1) (2018) 1-14.
- [42] Li B., Shan C.-L., Zhou Q., Fang Y., Wang Y.-L., Xu F., Han L.-R., Ibrahim M., Guo L.-B., Xie G.-L., Synthesis, characterization, and antibacterial activity of cross-linked chitosan-glutaraldehyde, *Marine Drugs* 11(5) (2013) 1534-1552.
- [43] Dwivedi R., Singh A.K., Dhillon A., pH-responsive drug release from dependal-M loaded polyacrylamide hydrogels, *Journal of Science: Advanced Materials and Devices* 2(1) (2017) 45-50.
- [44] Khan S., Ranjha N.M., Effect of degree of cross-linking on swelling and on drug release of low viscous chitosan/poly(vinyl alcohol) hydrogels, *Polymer Bulletin* 71(8) (2014) 2133-2158.
- [45] Stulzer H.K., Lacerda L., Tagliari M.P., Silva M.A.S., Fávère V.T., Laranjeira M.C.M., Synthesis and characterization of cross-linked malonylchitosan microspheres for controlled release of acyclovir, *Carbohydrate Polymers* 73(3) (2008) 490-497.
- [46] Desai K.G.H., Park H.J., Preparation of cross-linked chitosan microspheres by spray drying: Effect of cross-linking agent on the properties of spray dried microspheres, *Journal of Microencapsulation* 22(4) (2005) 377-395.

## التعديل الكيميائي مع التشخيص للكيتوسان للتطبيقات الصيدلانية

محمد ع. المعلا\*<sup>1</sup>, مازن ن. موسى<sup>1</sup>, محمد ستار<sup>2</sup>

<sup>1</sup> فرع الكيمياء الصيدلانية، كلية الصيدلة، جامعة البصرة، البصرة، العراق

<sup>2</sup> فرع الصيدلانيات، كلية الصيدلة، جامعة البصرة، البصرة، العراق

### الخلاصة

تم تحضير تسعة من مشتقات الكيتوسان المتشابهة (CLCS) باستخدام ثلاثة أنواع مختلفة من الروابط الشابكية: الجلوتارالدهيد والجليوكسال والتريفلالديهيد. تم استخدام CLCS المحضر للتحكم في إطلاق دواء الأسيكلوفير (ACV) من أجل تحسين التوافر البيولوجي للأسيكلوفير عن طريق الفم. تم تحضير CLCS من خلال التفاعل القائم على (قاعدة شيف) وتم تشخيصها عن طريق التحليل الطيفي للأشعة تحت الحمراء (FTIR)، وقياسات حيود الأشعة السينية، والفحص الحراري الوزني، والمسح التفاضلي، والمسح المجهر الإلكتروني (SEM). تم إثبات إنشاء رابطة الامين (C = N) في FTIR. مقارنةً بالكيتوسان الخام، أظهرت مشتقات الكيتوسان المتشابهة بنية غير متبلورة وأظهرت قدرة أكبر على الاحتفاظ بالمياه تزداد مع زيادة نسبة المادة الرابطة. أبرز الفحص المجهر الإلكتروني للمشتقات المتشابهة مناطق ذات أسطح خشنة وأخاديد لم تكن موجودة في سطح الكيتوسان الأصلي. كما تم فحص الاختلاف في درجة الانتفاخ مع اختلاف كمية المادة الرابطة. أبدى الكيتوسان المتشابه انتفاخاً أقل وكانت درجة الانتفاخ تتناقص مع زيادة كثافة المادة الرابطة. تم اختبار CLCS المحضرة في التحكم في تحرير عقار الأسيكلوفير من خلال دمجه مع الدواء على شكل حبيبات ثم وضع الحبيبات في جهاز تحرير الدواء. أظهرت نتائج تحرير الدواء في المختبر إطلاقاً مستداماً لـ ACV متأثراً بنوع ونسبة المادة الرابطة المستخدمة.